Chemical Engineering Journal 498 (2024) 155292

Contents lists available at ScienceDirect

Chemical Engineering Journal

journal homepage: www.elsevier.com/locate/cej

Denitrifying communities enriched with mixed nitrogen oxides preferentially reduce N_2O under conditions of electron competition in wastewater

Jinyu Ye [a,b], Marlene Mark Jensen [b], Estelle M. Goonesekera [b], Ran Yu [c], Barth F. Smets [b,d], Borja Valverde-Pérez [b,*], Carlos Domingo-Félez [b,e]

[a] School of Civil Engineering and Architecture, Zhejiang-Singapore Joint Laboratory for Urban Renewal and Future City, Zhejiang University of Science and Technology, Hangzhou, Zhejiang 310023, PR China
[b] Department of Environmental and Resource Engineering, Technical University of Denmark, DTU, Building 115, Bygningstorvet, Lyngby 2800, Denmark
[c] School of Energy and Environment, Wuxi Engineering Research Center of Taihu Lake Water Environment, Southeast University, Nanjing, Jiangsu 210096, PR China
[d] Center for Water Technology (WATEC), Department of Biological and Chemical Engineering, Ole Worms Alle 3, Aarhus University, Aarhus C 8000, Denmark
[e] James Watt School of Engineering, University of Glasgow, G12 8QQ, United Kingdom

ARTICLE INFO

Keywords:
Nitrous Oxide
Denitrification
Electron competition
Greenhouse gas emissions

ABSTRACT

The reduction rate of nitrous oxide (N_2O) is affected by the electron competition among the four denitrifying steps, limiting the mitigation of N_2O emissions during wastewater treatment. We foresee essential to understand how combinations of electron acceptors (EAs) affect the microbial composition and reduction mechanisms of denitrifying communities. We enriched three denitrifying communities from activated sludge biomass with equivalent loads of different EAs: NO_3^- (R1), N_2O (R2), and NO_3^- + N_2O (R3). The resulting enrichments were compared in terms of (1) reduction of nitrogen oxides in absence/presence of other EAs (NO_3^-, NO_2^-, N_2O), (2) their denitrification gene composition and (3) their microbial community composition. Batch results showed the presence of NO_3^- and NO_2^- suppressed N_2O reduction rates in all three reactors. The effect was lower in the mixed-substrate feed community than in the single-substrate feed under infinite sludge retention time and chemostat operation modes. N_2O-reducers of type *nosZ* II were enriched when N_2O serves as the sole EA, whereas *nosZ* I type N_2O-reducers were more prone to enrichment with NO_3^- as EA. The EA composition rather than the sludge retention mode differentiated the microbial communities. The genus *Flavobacterium* seems to play a significant role in alleviating the suppression of the N_2O reduction rate caused by electron competition. Limited conditions of electron supply are the norm independently of high C/N levels, and a community co-enriched with NO_3^- and N_2O alleviates more the competition for electrons in the nitrous oxide reductase enzyme than communities enriched with NO_3^- or N_2O individually.

1. Introduction

Nitrous oxide (N_2O) is a potent greenhouse gas with a global warming effect 300 times stronger than carbon dioxide (CO_2) and is also the most important ozone-depleting gas [1]. Biological nitrogen removal (BNR) by nitrification and denitrification has been recognized as an important source of N_2O emissions in wastewater treatment plants (WWTPs). The Intergovernmental Panel on Climate Change (IPCC) estimated that N_2O emissions in WWTPs reached 1.6 % of the total nitrogen load in 2019 [2]. Nitrous oxide accumulates in wastewater during BNR processes and is mainly produced biologically [3]. Denitrification describes the reduction of nitrate (NO_3^-) to dinitrogen (N_2) by heterotrophic denitrifying bacteria (HB), with nitrite (NO_2^-), nitric oxide (NO), and nitrous oxide (N_2O) as obligatory intermediates [4]. In addition, the abiotic reactions in the BNR system will also produce N_2O, but usually contribute little (<3 %) to overall N_2O emissions in BNR systems operated at standard pH and NO_2^- levels [5].

Heterotrophic denitrification is recognized as the only biological pathway for N_2O reduction [6]. Most studies focused on developing strategies to minimise N_2O emissions by decreasing net N_2O production

* Corresponding author at: Department of Environmental and Resource Engineering, Technical University of Denmark, DTU, Building 115, Bygningstorvet, Lyngby 2800, Denmark.
E-mail address: bvape@dtu.dk (B. Valverde-Pérez).

https://doi.org/10.1016/j.cej.2024.155292
Received 25 February 2024; Received in revised form 8 August 2024; Accepted 25 August 2024
Available online 30 August 2024

[7–9], while fewer focused on increasing the N_2O reduction to N_2 potential. For example, extending the duration of the anoxic phase to enhance the consumption of N_2O by HB could serve as a potential method to regulate anoxic accumulation of N_2O [3]. Importantly, the maximum N_2O reducing capacity of denitrifying microbial communities exceeds their capacity to produce N_2O by a factor of 2–10 fold [10], making denitrification a potential N_2O sink in wastewater treatment systems, scavenging N_2O derived from biological and abiotic reactions. Hence, increasing the N_2O reduction capacity may be an effective N_2O mitigation strategy.

In WWTPs, a variety of electron acceptors (EAs) coexist and competition for electrons occurs during denitrification [11]. Most denitrifying bacteria will prioritize the higher energy yield of reducing NO_3^- to N_2O rather than N_2O to N_2 (20 % efficiency difference) [1]. Thus, electron competition can increase the potential of N_2O accumulation and leads to incomplete denitrification, resulting in N_2O emissions as the end-product [12,13]. Studies conducted on denitrification communities enriched with acetate, ethanol, or methanol as the sole electron donor (ED) suggested that the potential N_2O reduction rate decreased more than 50 % when other EA (NO_3^- or NO_2^-) were present [14]. In single denitrifying biofilm systems a greater N_2O accumulation due to electron competition was more pronounced than in biofilm/flocs systems, and was associated to substrate diffusion limitations [11]. Current studies focused on the effect of different EDs or biotechnologies (e.g., activated sludge, granular sludge, biofilms), with limited insights into the effect of multiple EAs on denitrifying communities [15].

All denitrifying enzymes must compete for electrons from a shared electron supply system in the denitrification process. The nitrate reductase enzyme (NAR) receives electrons from the quinone pool and is located in the cytoplasm (NarG), while nitrite, nitric oxide, and nitrous oxide reductases (NIR, NOR, and NOS) obtain electrons from cytochrome c550 (Cytc 550), and are located outside (NIR, NOS) or in the membrane (cNOR) [16]. Due to the limited electron supply from Cytc 550, a strong competition for electrons exists among NIR, NOR, and NOS [14,17]. Nitrous oxide reductase (NOS) is the only known enzyme to reduce N_2O to N_2 [18]. The enzyme is encoded by the *nosZ* gene. Phylogenetic analysis revealed two major *nosZ* genotypes in prokaryotes, called clade I (*nosZ* I) and II (*nosZ* II) [19]. The abundance of bacteria carrying clade *nosZ* I or *nosZ* II changed with the dilution rate and EA/ED ratio in a chemostat with N_2O as the sole EA [20,21]. N_2O-reducing bacteria that possess clade II type *nosZ* may thrive over clade I type *nosZ* because the former has higher growth yields and a lower N_2O affinity constant [22]. A higher biomass yield implies a greater efficiency of energy conservation in the *nosZ* II −associated electron transport chain, whereas a lower affinity constant would confer *nosZ* II type N_2O reducers a selective advantage during competition for limiting amounts of N_2O [21,23]. Exploring the factors driving the enrichment of *nosZ* clade I and II microorganisms under relevant EA abundances is particularly important. Considering the diverse denitrification gene cassettes in HB and their distinct affinities for EAs, we hypothesize that under conditions of electron competition bacteria enriched with multiple EAs favour N_2O reduction compared to enrichments solely fed with N_2O.

Hence, our goal was to investigate the feasibility of enriching N_2O consumers that preferentially utilise N_2O when multiple EAs coexist, especially in the presence of NO_3^-, the most abundant EA in mixed liquor. To achieve this goal, three chemostats were fed acetate as the sole ED and with equivalent loads of NO_3^-, N_2O, or NO_3^- + N_2O. Differences in potential N_2O reduction and electron consumption rates under electron competition conditions were elucidated. The abundance of denitrification genes and the microbial community structure of three enrichments are also reported in order to associate differences in N-consumption rates to community variations.

2. Materials and methods

2.1. Reactor set-up and operation

The seeding material was collected from the secondary sedimentation tank in the activated sludge line of Mølleåværket WWTP (Kgs. Lyngby, Denmark). The experiments were carried out in three reactors (R1, R2, and R3) with a working volume of 1 L (Fig. 1). The reactors were operated without headspace to prevent gas accumulation and pressure imbalances during operation. The hydraulic retention time (HRT) was set to 1.54 days to support the growth, under chemostat operation, of *nosZ II* type N_2O reducers, vital for effective N_2O reduction [20]. A peristaltic pump supplied synthetic wastewater to the system to dilute the medium. The reactors were operated at room temperature (20–26 °C). To ensure anoxic conditions essential for denitrification, the synthetic wastewater was pre-sparged with N_2 before entering the reactors, eliminating any dissolved oxygen (DO). The DO concentration and pH were monitored continuously (WTW GmbH, Weilheim, Germany), the former to ensure anoxic conditions with DO levels below the detection limit of the sensor. The operation period was divided in 2 phases: 1) infinite sludge retention time (SRT) (Day 0–42), during which effluent sludge was returned to the reactor every 2 days; and 2) chemostat operation (HRT equal to SRT, Day 42–77). The two operation modes favour slow-growing and fast-growing microbes respectively.

The synthetic wastewater contained 30 mg-eq EA/L, 200 mg-COD/L as sodium acetate, NH_4Cl 11.5 mg/L, KH_2PO_4 10 mg/L, $MgSO_4{\cdot}7H_2O$ 10 mg/L, and 2.5 mL/L trace element solution. In R1 NO_3^- was the only EA (6 mg-N/L), in R2 N_2O (30mgN-L), and in R3 an equivalent load of NO_3^- (3 mg-N/L) and N_2O (15 mg-N/L). Hence, the three reactors received the same load of EAs at non-limiting C/N ratio, with varying loads for each enzyme: the NAR and NOS enzymes receive 40 % and 20 % of the electrons in R1, compared to 0 % and 100 % in R2, and 20 % and 60 % in R3. The target N_2O liquid concentration in synthetic wastewater was obtained by bubbling gas with composition of 5 % N_2O and 95 % N_2 for specific time intervals (Fig S1). Synthetic wastewater was prepared every 2 days, ensuring stable N_2O levels as supported by stability tests showing that the N_2O concentration decreased by less than 10 % within this period (Fig. S1). The trace metal solution contained (g/L): 50.0 g ethylenediamine tetraacetic acid, 8 g $FeCl_3$, 0.15 g H_3BO_3, 0.15 g $CoCl_2{\cdot}6H_2O$, 0.12 g $CuSO_4{\cdot}5H_2O$, 0.12 g $MnCl_2{\cdot}4H_2O$, 0.12 g $ZnSO_4{\cdot}7H_2O$, 0.12 g $Na_2MoO_4{\cdot}2H_2O$ and 0.12 g $NaSeO_4{\cdot}10H_2O$ in 1 L of water.

2.2. Batch tests – Potential denitrification rates

Batch tests were carried out to quantify reduction rates of NO_3^-, NO_2^-, and N_2O in R1, R2, and R3 at the end of both growth modes (days 42 and 77). Seven types of batch tests (A-G) were conducted using single, binary, and tertiary mixtures of NO_3^-, NO_2^-, and N_2O (Table 1). Biomass from each bioreactor was concentrated to 0.5 gVSS/L (infinite SRT) or 0.25 gVSS/L (chemostat), aerated for one hour to oxidize intracellular COD, and sparged with N_2 gas for 5 min to ensure anoxic conditions. The pH was controlled at 7.5 ± 0.1 by addition of 1 M NaOH or 1 M HCl at the beginning of the test.

Nitrogen oxides were added initially (Table 1), followed by 300 mg-COD/L (non-rate-limiting concentration). In the cases where N_2O was used as the EA, N_2O was added first to obtain a stable signal from the liquid microsensor to confirm the initial concentration (N_2O-R, Unisense, Aarhus, Denmark). Batch tests were conducted as triplicates. Mixed liquor volatile suspended solids (MLVSS; an estimate of biomass concentration) was determined at the end of the incubations.

2.3. Reaction and electron uptake rates

Rates of NO_3^-, NO_2^- and N_2O reduction were calculated by linear regression of the concentration of NO_3^-, NO_2^- and N_2O over time. Rates

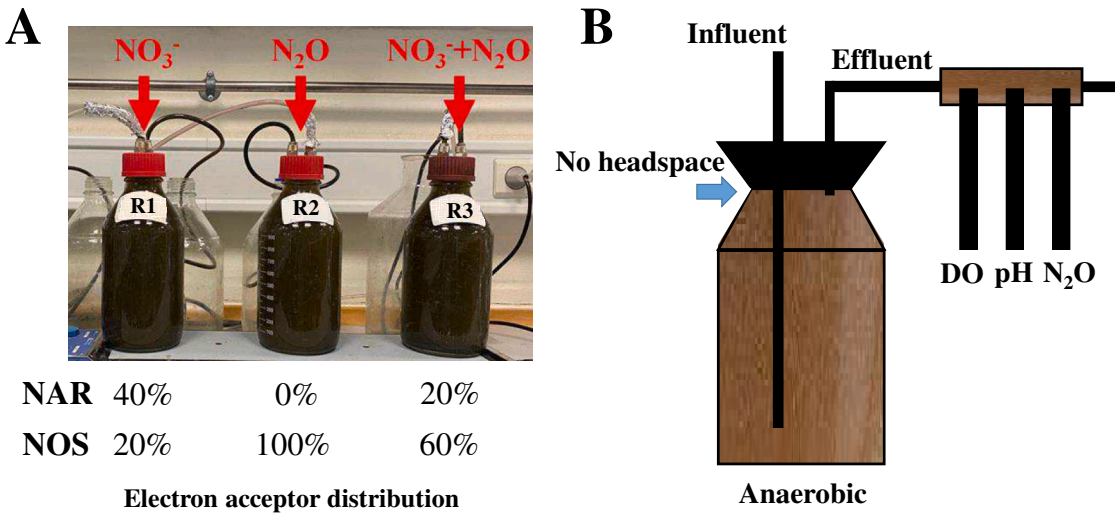

Fig. 1. The experimental setup (A) and the schematic diagram of the bioreactor (B).

Table 1
Batch experiments conducted for each set of tests at the end of infinite SRT and chemostat operation phases (days 42 and 77).

ID	Electron Acceptors (EAs) added	Measurements
A	NO_3^- (30 mg–N/L)	NO_3^--N
B	NO_2^- (30 mg–N/L)	NO_2^--N
C	N_2O (30 mg-N/L)	N_2O-N
D	NO_3^- + NO_2^- (30 mg-N/L+30 mg-N/L)	NO_3^--N and NO_2^--N
E	NO_3^- + N_2O (30 mg-N/L+30 mg-N/L)	NO_3^--N and N_2O-N
F	NO_2^- + N_2O (30 mg-N/L+30 mg-N/L)	NO_2^--N and N_2O-N
G	NO_3^- + NO_2^- + N_2O (30 mg-N/L+30 mg-N/L+30 mg-N/L)	NO_3^--N, NO_2^--N and N_2O-N

are expressed as maximum rates ($NO_{3,m}^-$, $NO_{2,m}^-$, and $N_2O_{,m}$) per gram VSS. The reduction rate of nitrogen oxide (NO_x) was calculated as follows:

$$rNO_3^- = rNO_{3,m}^- \quad (1)$$

$$rNO_2^- = rNO_{2,m}^- + rNO_3^- \quad (2)$$

$$rNO = rNO_{,m} + rNO_2^- \quad (3)$$

$$rN_2O = rN_2O_{,m} + rNO \quad (4)$$

where rNO_3^-, rNO_2^-, rNO and rN_2O (mg-N/(g-VSS·h)) are the reduction rates of NO_3^-, NO_2^-, NO and N_2O, respectively. Nitric oxide (NO) is assumed to be turned over fast and therefore equivalent to the reduction rate of NO_2^-, thus rNO=rNO_2^-.

The electron consumption rate by each step of denitrification was calculated as follows:

$$rNar - e = rNO_3^-/14 \times 2 \quad (5)$$

$$rNir - e = rNO_2^-/14 \times 1 \quad (6)$$

$$rNor - e = rNO/14 \times 1 \quad (7)$$

$$rNos - e = rN_2O/14 \times 1 \quad (8)$$

where rNar-e, rNir-e, rNor-e, and rNos-e (mmol e^-/(gVSS·h)) are the electron consumption rates of Nar, Nir, Nor and Nos, respectively.

2.4. Microbial characterization

Samples for DNA extraction were collected at the beginning of the incubations and the end of both the infinite SRT and chemostat operations. The samples were frozen immediately at −20 °C until extraction. According to the manufacturer's instructions, DNA was extracted using Fast DNASPIN^{TM} Kit for soils (MP Biomedicals, OH, USA). The quantity and quality of the extracted DNA were measured and checked by its 260/280 nm wavelength ratio (NanoDrop, ThermoFisher Scientific, TN, USA).

Quantitative PCR analysis was used to target and quantify specific genes in the individual steps in the denitrification pathway and 16S rRNA of *Eubacteria*. The SYBR fluorogenic PCR method was used on Roche LightCycler 96 (Mannheim, Germany). All samples and controls were measured in duplicates. The relative abundance of each functional gene was normalized based on the total abundance of 16S rRNA gene. Primers and conditions used for quantification of each gene are listed in Table S1.

DNA amplification and sequencing were modified based on a previously reported method [24]. DADA2 version 1.16 was used for the generation of amplicon sequence variants (ASVs), which were compared with SILVA SSU Database v138 for the taxonomic assignment of 16 S rRNA genes Sequence analyses were carried out using the analytical software in Majorbio I-Sanger Cloud (v2.0, https://www.i-sanger.com). A principal coordinate analysis (PCoA) was generated according to the Bray-Curtis distance matrix using the full set of OTUs from each sample. Sequence data can be found in the NCBI database under the BioProject reference PRJNA1066232.

2.5. Analytical methods and statistical analysis

Before COD and nitrogen species analysis, liquid effluent samples were filtered through 0.45 μm pore size filters (Agilent Technologies, CA, USA). The COD was measured using a COD digestion kit (2125815, Hach Company, CO, USA). Bulk NO_3^- and NO_2^- were analysed colorimetrically by a continuous-flow auto-analyser (SKALAR Santt, Breda, Netherlands). Total VSS were assayed using a filter paper with a pore size of 0.45 μm (Whatman, Maidstone, UK).

All tests were performed in triplicate, and the results were expressed as the mean ± standard deviation. An analysis of variance (ANOVA) was applied to test the significance of the results, and $p < 0.05$ was considered significant.

3. Results and discussion

3.1. Reactor performance under continuous operation

During continuous operation nitrogen oxides were not detected in the effluent. At the same time, the COD concentration were 73 ± 4.6

mg/L and 158 ± 3.7 mg/L during infinite SRT and chemostat operation respectively (Fig. 2), indicating sufficient COD loading as ED to support complete denitrification. The consumption of COD was significantly higher in the infinite SRT period (Days 0–42) than during the chemostat operation (Days 42–77) in all three reactors, corresponding to the relatively higher level of biomass during the infinite SRT period, ranging between 0.45 ± 0.08 (R2) and 0.68 ± 0.03 g/L (R1) (Fig. 2). Despite the limited availability of EAs in both periods, the longer SRT allowed microorganisms more time to uptake organic matter, resulting in higher COD removal and increased biomass [25]. However, the effluent COD measurements cannot elucidate the fraction of acetate to soluble inert COD in the effluent.

Even though the three reactors received the same load of EAs, the VSS in R2 with N_2O as the sole EA was consistently lower than in R1 and R3 under infinite SRT, suggesting a relatively lower biomass yield. The reduction of NO_3^- involves multiple steps, and a longer chain will likely be thermodynamically more efficient, resulting in higher biomass yield [26]. In contrast, the reduction of N_2O is a single-step process, facilitating faster but less efficient process. Therefore, during N_2O reduction, more organics are used for energy metabolism instead of contributing to increased biomass yield [20]. Upon entering the chemostat operation, the VSS in the three reactors rapidly decreased to approximately 0.07 ± 0.01 g/L with no significant differences between the three reactors. This change was attributed to the lower SRT and the limitation of microbial growth due to restricted EA supply, leading to reduced VSS [27]. However, the cell yield could not be differentiated from other COD fractions in the biosolids such as sorption of decay products or storage of acetate. At nutrient-limiting conditions the sludge yield is expected to differ from non-limiting conditions due to acetate storage, and also vary between chemostat and infinite SRT operations [28,29].

3.2. Potential nitrogen oxides reduction in batch tests

The specific reduction rates of NO_3^-, NO_2^-, and N_2O within single-substrate batches (A, B, and C) significantly differed between the infinite SRT and chemostat operations for R1, R2, and R3 (Table 2). After the period of infinite SRT (day 42), the reduction rates of NO_3^-, NO_2^-, and N_2O in the three enrichments were 3.2 ± 0.3 – 5.8 ± 0.9 mg-N/g-VSS·h, 4.9 ± 0.5 – 6.6 ± 1.3 mg-N/gVSS·h, and 31.3 ± 1.2 – 33.6 ± 1.9 mg-N/gVSS·h, respectively (Fig. 3, S2, S3). Reduction rates were generally lower than those in the chemostat operation (day 77) (5.9 ± 1.1 – 9.3 ± 1.8 mg-N/gVSS·h, 6.4 ± 1.4 – 12.8 ± 2.3 mg-N/gVSS·h, and 45.1 ± 2.3 – 77.7 ± 3.1 mg-N/gVSS·h) [30]. During the infinite SRT period, the accumulation of low activity biomass may lead to a reduction in the denitrification rate relative to VSS. Conversely, during the chemostat operation with shorter SRT, a higher cell activity is expected,

Table 2
Reduction rates of NO_3^-, NO_2^-, and N_2O in batch test experiments A, B, and C.

		Reduction rates for nitrogen oxides (mg-N/gVSS·h)		
	EA	R1 (NO_3^-)	R2 (N_2O)	R3 (NO_3^-+ N_2O)
Infinite SRT	NO_3^-	5.8 ± 0.9	3.2 ± 0.3	4.6 ± 0.7
	NO_2^-	6.6 ± 1.3	4.9 ± 0.5	5.0 ± 0.8
	N_2O	31.5 ± 2.1	33.6 ± 1.9	31.3 ± 1.2
Chemostat	NO_3^-	9.3 ± 1.8	5.9 ± 1.1	8.0 ± 1.5
	NO_2^-	12.8 ± 2.3	6.4 ± 1.4	9.8 ± 1.9
	N_2O	45.1 ± 2.3	77.7 ± 3.1	56.4 ± 2.4

reflecting a more active microbial community [31]. In R1, NO_3^- and NO_2^- reduction rates are generally higher than R2 and R3. The reduction rate of N_2O is much higher than NO_3^- and NO_2^- in all enrichments, which is consistent with the work of Conthe et al. (2019), who showed that the ability of denitrifying communities to reduce N_2O is always in excess as compared to NO_3^- or NO_2^- [10]. During the chemostat operation, the N_2O reduction rate in R2 reached 77.7 ± 3.1 mg-N/gVSS·h, significantly surpassing the rates in R1 (45.1 ± 2.3 mg-N/gVSS·h) and R3 (56.4 ± 2.4 mg-N/gVSS·h). In R2, under chemostat conditions, microorganisms capable of N_2O reduction possibly gained an ecological advantage. This selective pressure led to the highest N_2O reduction rate in R2 under limited SRT conditions [32]. During the infinite SRT period the continuous accumulation of sludge in the system decreased the ecological differentiation. Although selective pressure also existed, it allowed all types of microorganisms to accumulate, including those with weaker N_2O reduction capabilities and active denitrifying pathways. A model denitrifier *Paracoccus denitrificans* synthesized NirS even when only fed N_2O, but to a lower level than fully active denitrifying cells. To synthesize a complete denitrifying proteome would waste energy, but was suggested as an investment for changing environmental conditions, as seen by the slightly lower denitrification rates when N_2O was fed as compared to NO_3^- and NO_3^- + N_2O (Fig. 3) [33].

3.3. Electron competition during batch tests

In order to investigate the electron competition in the three reactors under the coexistence of EAs, we designed seven different batch experiments with various EA combinations (Table 1). When two or more EAs were available at non-rate-limiting concentrations, the reduction rate of nitrogen oxides generally decreased, regardless of the biomass retention mode (Fig. 3) [34]. In the D – G groups, the reduction rates of NO_3^- and NO_2^- declined by 14.9 % – 46.7 % and 9.2 % – 46.4 %, respectively, compared to batches where only one type of nitrogen oxide was added, while the N_2O reduction decreased by 18.1 % – 55.4 %. The lower reduction rates reveal the competition for electrons during

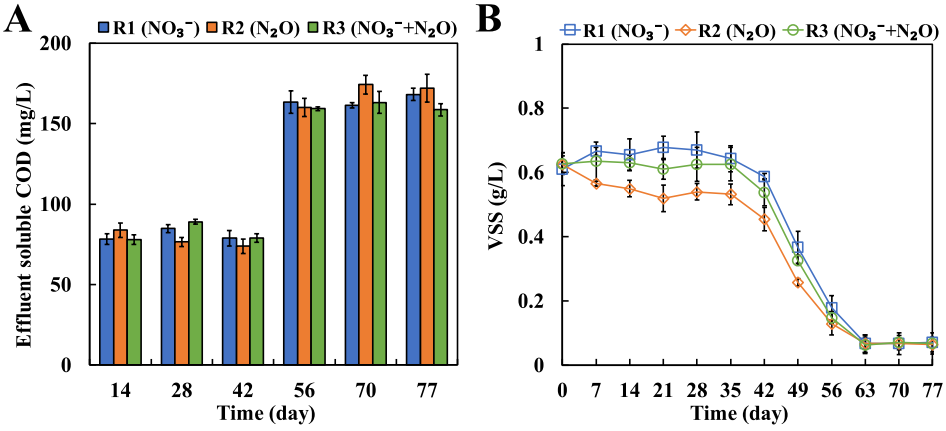

Fig. 2. Concentrations of soluble COD in the effluent (A) and biomass concentration in the reactors (B) of R1, R2, and R3. Nitrogen oxides in the effluent were below detection limit during operation (<0.1 mg-N/L).

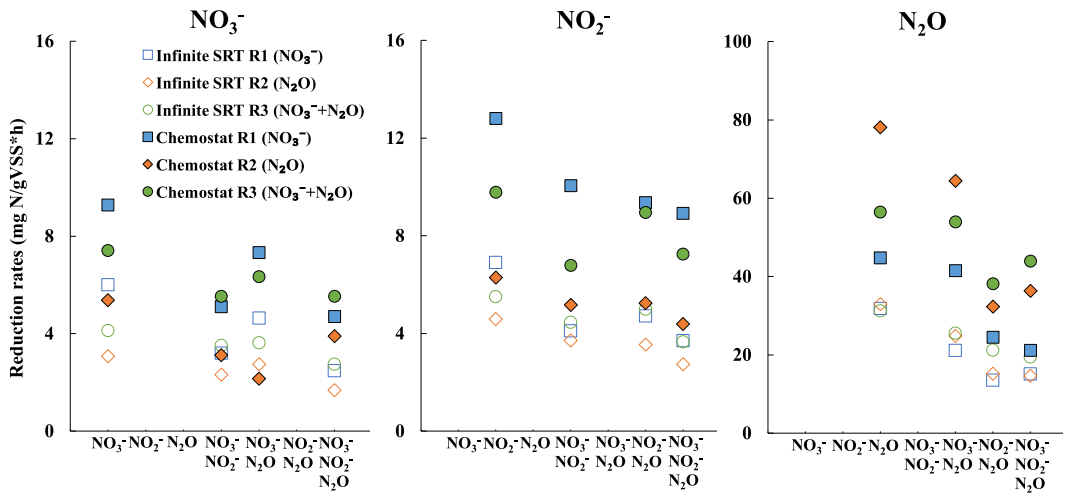

Fig. 3. Reduction rates of NO_3^-, NO_2^-, and N_2O in batch tests A-G during infinite SRT and chemostat growth modes (day 42 and 77 respectively).

denitrification and highlight the preference for NO_3^- and NO_2^- reduction over N_2O. The preferential selectivity of EA may be due to the bio-energetic properties of denitrifying bacteria, where most of the energy is lost in the NO and N_2O reduction steps of denitrification [16]. In fact, approximately 80 % of ATP is produced during the reduction of NO_3^- to N_2O, and the further reduction of N_2O to N_2 contributes relatively little to the total energy output of microorganisms [1].

Sludge enriched with NO_3^- (R1) or N_2O (R2) exhibited lower N_2O reduction rates in the presence of other EAs compared to sludge concurrently enriched with NO_3^- and N_2O (R3) in both the infinite SRT and chemostat operation (Table 3). The N_2O reduction rate in groups F and G in R1 and R2 was suppressed by 52.3 ± 6.4 % − 57.6 ± 6.8 % and 45.2 ± 7.2 % − 58.6 ± 8.9 %, respectively, which was significantly higher than the corresponding N_2O reduction rate inhibition in R3 (32.1 ± 5.8 % − 37.7 ± 5.9 % and 22.1 ± 6.5 % − 32.3 ± 4.2 %). The R3 community increased N_2O reduction under conditions of high competition for electrons. In R3, when NO_3^- and N_2O coexist, although the reduction of NO_3^- can generate more energy, N_2O corresponds to 60 % of the EA load, and the microbial community's adaptation to this electron-competitive environment ensures the effective reduction of N_2O [35]. The co-expression of NAR and NOS was suggested advantageous as a bet-heding strategy to save energy, which would be triggered by the presence of NO_3^- and N_2O [33]. In contrast, in the R1 community the maximum NO_3^- reduction limits the supply of EAs to the consecutive reduction rates. The R2 community is only exposed to the last NO_x, and co-expressing the complete enzymatic cascade would not make bio-energetic sense.

In the infinite SRT period, the N_2O reduction rates in R1, R2, and R3 in the presence of NO_3^- are inhibited by 33.7 %, 24.7 %, and 18.1 %, respectively. However, during the chemostat operation, the inhibition rates of their N_2O reduction rates decreased to 7.2 %, 17.5 %, and 4.2 %, respectively. Due to the accelerated loss of biomass during the chemostat operation, microorganisms are selected for faster growth and metabolic rates. Under this environmental stress, microorganisms may need to utilize all available EAs, including NO_3^- and N_2O, to maximize energy production, and thus, a lighter inhibition of the N_2O reduction rate was observed at this stage. In test groups where only NO_2^- was added or NO_3^- was mixed with NO_2^-, the inhibition of N_2O reduction rate was generally higher than in the groups where only NO_3^- was added, with inhibition rates ranging from 32.1 ± 5.8 % to 58.6 ± 8.9 % and 22.1 ± 6.5 % to 55.4 ± 6.4 %, respectively. This significant suppression effect is likely since the enzymes responsible for NO_2^- reduction (NIR), along with NOS, are located in the periplasm of the cell, and they both acquire electrons from the same cytochrome pool, compared to the periplasmic NarG from quinones (Fig. 4A). Generally, in the same test group, the decrease of N_2O reduction rate in the chemostat derived culture was lower than that in the infinite SRT period, which can be attributed to the competitive advantage induced by EA limitation in the chemostat operation [12]. Therefore, the N_2O reduction rate in the denitrifying community enriched under coexistence of EAs (R3) was less inhibited by electron competition.

Table 3
Inhibitory effect of electron competition on N_2O reduction rate in batch test experiments E, F, and G.

		N_2O reduction rate inhibition (%)		
	EA	R1 (NO_3^-)	R2 (N_2O)	R3 (NO_3^-+ N_2O)
Infinite SRT	NO_3^- + N_2O	33.7 ± 8.8	24.7 ± 6.4	18.1 ± 5.5
	NO_2^- + N_2O	57.6 ± 6.8	53.9 ± 6.3	32.1 ± 5.8
	NO_3^-+NO_2^- + N_2O	52.3 ± 6.4	55.4 ± 6.4	37.7 ± 5.9
Chemostat	NO_3^- + N_2O	7.2 ± 4.4	17.5 ± 6.7	4.3 ± 2.4
	NO_2^- + N_2O	45.2 ± 7.2	58.6 ± 8.9	32.3 ± 4.2
	NO_3^-+NO_2^- + N_2O	52.6 ± 7.4	53.5 ± 5.5	22.1 ± 6.5

3.4. *Effect of SRT on electron competition in denitrifying sludge*

Under the infinite SRT period, the maximum electron consumption rates of NO_3^- reductase (NAR), NO_2^- reductase (NIR), NO reductase (NOR), and N_2O reductase (NOS) in R3 are 0.59, 0.36, 0.36, and 2.12 mmol e/(gVSS·h) respectively (Fig. 4B). However, during the chemostat operation, the maximum electron consumption rates increased to 1.06, 0.70, 0.70, and 4.03 mmol e/(gVSS·h) respectively. The longer biomass retention time during the infinite SRT period may result in lower specific electron consumption rates due to accumulation of inactive or non-denitrifying biomass. Conversely, biomass retention time is reduced during the chemostat operation, selecting fast growing microorganisms, leading to higher specific electron consumption rates.

The competition among all denitrifying enzymes persists even under non-limiting organic carbon supply conditions (Fig. 4A). Specifically, NAR receives electrons from the quinone pool, while NIR, NOR, and NOS obtain electrons from the same cytochrome, c550 (Cytc 550) [14,17]. The larger reduction of NOS activity in the presence of NO_2^- compared to NO_3^- could be caused by electron competition rather than enzymatic inhibition. During the infinite SRT period, the sum of the maximum electron consumption rates that denitrifying enzymes can achieve independently in R3 is 3.43 mmol e/(gVSS·h) (Single substrate batches: A-NAR, B-NIR, C-NOS). This is notably higher than the corresponding electron consumption rate in batch G (NO_3^- + NO_2^- + N_2O) of 2.96 mmol e/(gVSS·h), indicating the occurrence of electron

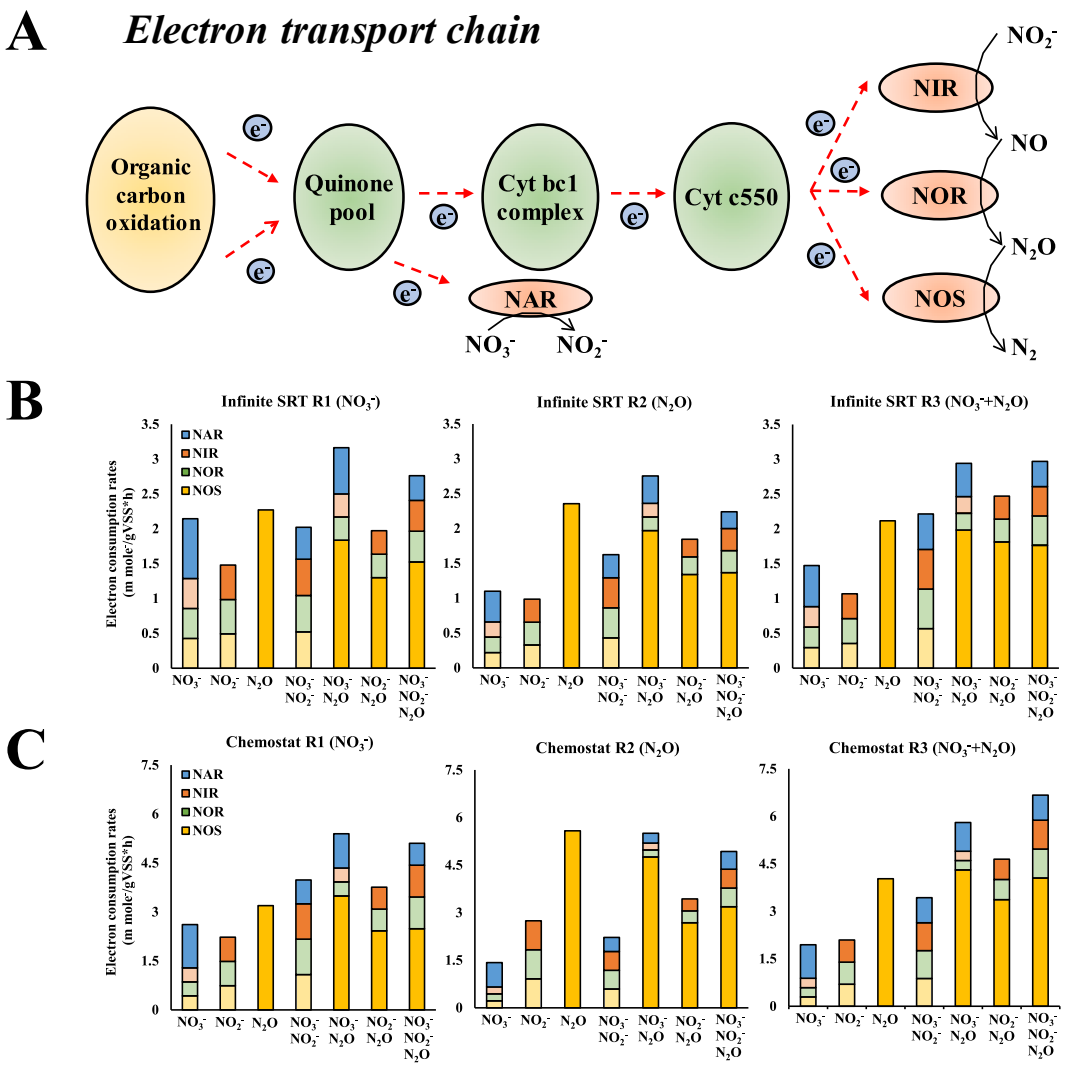

Fig. 4. Schematic diagram of the electron transfer chain (A) and electron consumption rates of different denitrifying enzymes at infinite solid retention time (B) and chemostat operation (C). Shaded areas correspond to unmeasured rates.

competition. However, during the chemostat operation, the sum of the potential denitrifying enzymes' electron consumption rates in R3 (G) is 6.5 mmol e/(gVSS·h), nearly matching the maximum electron consumption rate of 6.7 mmol e/(gVSS·h). The denitrifying community enriched under the EA mixture may have optimized against electron competition among different denitrifying enzymes via specific internal regulatory mechanisms, enabling the overall electron consumption rate to approach their individual potential electron consumption rates. In batch test A of R3, the electron consumption rates of NAR during the infinite SRT and chemostat operation were 0.59 mmol e/(gVSS·h) and 1.06 mmol e/(gVSS·h), respectively. However, in tests D and E, the electron consumption rates of NAR decreased to 0.51–0.48 mmol e/(gVSS·h) and 0.79–0.91 mmol e/(gVSS·h), respectively. This suggests that the coexistence of other EAs such as NO_2^- or N_2O may select for denitrifying microbial communities that favourably utilize these EAs. Observations in denitrifying polyphosphate accumulating organism (dPAO) communities further support this adaptability in electron distribution and utilization [17]. This adaptability enables microorganisms to effectively allocate and optimize energy based on available resources, particularly under continuously changing environmental conditions.

In R1, R2, and R3, the NOS electron consumption rates in NO_2^- added batch tests (F and G) were 1.30–2.48 mmol e/(gVSS·h), 1.34–3.19 mmol e/(gVSS·h), and 1.76–4.05 mmol e/(gVSS·h) respectively, generally lower than in single substrate batch test C (2.12-2.36 mmol e/(gVSS·h) and 3.20–5.58 mmol e/(gVSS·h)), indicating that the electron competition caused by the addition of NO_2^- leads to a reduction in the electrons flowing to NOS. However, the combined addition of NO_3^- and N_2O in batch test E during chemostat operation showed NOS electron consumption rates of 3.5 mmol e/(gVSS·h) and 4.3 mmol e/(gVSS·h) in R1 and R3 respectively. Differently from batch test F and G with NO_2^-, the NOS consumption rate in presence of NO_3^- slightly exceeded those in the single substrate batch test C, which were 3.2 mmol e/(gVSS·h) and 4.0 mmol e/(gVSS·h). Such observations could be attributed to the microbial preference for NO_3^- utilization in R1 and R3, implying that electron competition from the quinone pool and Cytc 550 might not be as significant as within Cytc 550. In an SBR with denitrifying glycogen accumulating organisms, the addition of NO_3^- was also found to not affect the NOS electron consumption rate [17]. It is important to note that in R3, the electron consumption rates of NOS in tests E, F, and G were 1.98–4.31 mmol e/(gVSS·h), 1.81–3.37 mmol e/(gVSS·h), and 1.76–4.05 mmol e/(gVSS·h), respectively, significantly higher than in R1 (1.83–3.50 mmol e/(gVSS·h), 1.30–2.42 mmol e/(gVSS·h), 1.52–2.49 mmol e/(gVSS·h)). This phenomenon reflects the adaptability of the microbial community in R3 to the coexistence conditions of NO_3^-

and N_2O. The enriched microorganisms might prioritize transferring electrons to N_2O reduction in the presence of EA competition, leading to a higher proportion of electrons being consumed by NOS compared to those adapted to using only NO_3^- in denitrifying sludge. While around 70 % of the genomes carrying *nosZ* also carry the genes for NIR and NOR, the gene presence does not translate necessarily to activity, as active enzymes depend on gene transcription, translation and posttranslational modifications [33]. Furthermore, although the maximum electron consumption rate of NOS in R2 was 6.6 %-27.8 % higher than in R3, the inhibition rate of NOS was also higher, ranging between 26.7 %-75.4 % (Fig. 4 and Table 3). In denitrifying sludge where N_2O is the sole EA, theoretically, microorganisms should allocate more electrons to NOS.

Relevant conditions for wastewater treatment include nitrification products NO_3^- or NO_2^-, which trigger electron competition and reduce the electron flow to NOS, thereby increasing the inhibition rate of N_2O reduction. Therefore, in denitrifying sludge cultured with a mix of NO_3^- and N_2O (R3), the electron supply to NOS is less affected by electron competition, thus maintaining a higher consumption rate even under conditions of limiting electron supply.

3.5. Denitrification functional gene abundance

Compared to the original sludge, when NO_3^- was used as the sole EA there was a notable increase in the relative abundance of *narG*, *nirS*, and *nosZ* I genes within the total bacterial community, with increments of 48.1 %-51.9 %, 26.1 %-30.2 %, and 52.2 %-78.5 %, respectively (Fig. 5). Similarly, when NO_3^- and N_2O were jointly employed as EAs, the relative abundances of *nirS* and *nosZ* I genes also increased 32.1 %-40.8 % and 12.1 %-44.9 %, respectively, while the relative abundance of the *narG* gene did not show significant changes. However, under conditions where N_2O served as the sole EA, the community retained the denitrifying capability associated to *nosZ* I clade by also enriching for *nar* and *nir* genes. The relative abundance of the *nirS* gene in R2 decreased by 7.2 %-48.1 %, whereas the *nosZ II* gene's relative abundance significantly increased by 472.3 %-2379.1 %. Additionally, in the sludge samples from all three reactors, a substantial rise in the relative abundance of the *nirK* gene was observed, ranging from 226.6 % to 1347.1 %.

Specifically, in R2 and R3, during the infinite SRT period, the abundance of the *napA* gene as a proportion of the total bacteria is 5 times and 7.5 times higher, respectively, than during the chemostat operation. This indicates that *napA*-type denitrifiers grow slower than *narG*-type denitrifiers and are better adapted to longer sludge retention times. Furthermore, the *narG* gene in R1 accounted for 34.3 %-35.2 % of the total bacteria, which is generally higher than in R2 (23.2 %-29.5 %) and R3 (21.4 %–23.1 %), which may be due to the fact that R1 received the largest load of NO_3^-. As for the genes responsible for NO_2^- reduction, the *nirS* gene accounted for 4.2 %-12.3 % of the total bacteria, which is significantly higher than the *nirK* gene (0.1 %-0.5 %). Previous studies have also reported that *nirS* plays a dominant role in reducing NO_2^- to NO processes in activated sludge compared to *nirK* [36]. The proportion of the *nirS* gene in the total bacteria in R1 and R3, where NO_2^- was produced, was 11.1 % and 10.9 %, and 12.3 % and 12.1 % during the infinite SRT and chemostat periods. However, in R2 where N_2O was added as EA *nirS* accounted for 8.1 % and 4.3 %. Interestingly, the abundance of the *nirK* gene in R1 during the chemostat operation was 3.5 times higher than during the infinite SRT period, but still remained at much lower abundances than *nirS*.

For N_2O reducers, the proportion of the *nosZ* I gene of total bacteria in R1 and R3 (9.2 %-10.8 % and 6.8 %-8.8 %) is generally higher than that of *nosZ* II (0.6 %-1.0 % and 1.2 %-2.2 %). From microbial genomes carrying the *nosZ* I clade gene 83 % also carry other denitrification genes such as *narG*, *napA*, *nirS*, or *nirK*, making these microorganisms more likely to be complete denitrifiers [37]. This situation might lead to a higher observed abundance of the *nosZ* I clade gene in environments containing diverse EAs. Conversely, most microorganisms carrying the *nosZ* II clade gene appear to be primarily non-denitrifying N_2O reducers,

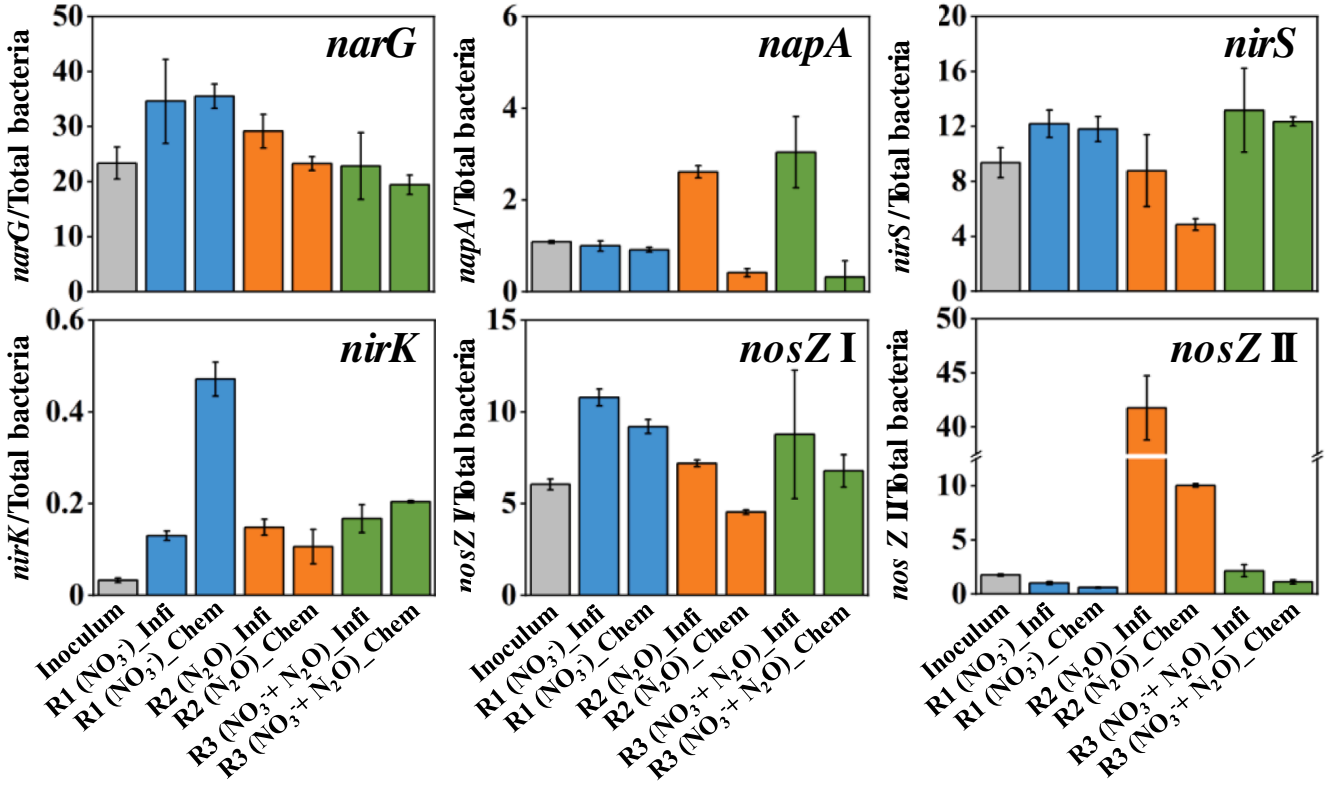

Fig. 5. Abundance of key denitrifying enzyme genes on the inoculum and by the end of the two operational periods.

forming a significant N_2O sink without participating in N_2O production [38,39]. In R2, we observed that the proportion of *nosZ* II type genes accounted for up to 41.8 % and 10.0 % in the infinite SRT and chemostat operation, respectively, demonstrating that *nosZ* II type denitrifiers are selected for in an environment where N_2O is the only EA. Previous studies also found that *nosZ* II type N_2O reducing microorganisms grow significantly under conditions where N_2O is the sole EA and growth limiting factor [21]. Therefore, the *nosZ* II type N_2O reducing microorganisms are predominantly enriched in denitrifying communities where N_2O serves as the sole EA, while the *nosZ* I type N_2O reducing microorganisms tend to enrich under conditions where NO_3^- is the sole or coexisting EA with N_2O.

3.6. Microbial community structure analysis

Supply of NO_3^-, N_2O, and NO_3^- + N_2O as EAs to R1, R2, and R3 enriched the inoculum sludge into different denitrifying communities. Based on the 16S rRNA gene library, the microbial community compositions of the three enriched cultures under two reactor operation modes were compared (Fig. 6). In the infinite SRT and chemostat operation, the Shannon indices (a metric for assessing microbial diversity) of denitrifying microbial communities enriched with NO_3^- were 3.9 and 4.2, respectively, slightly higher than the inoculum at 3.9 (Fig. S4). However, when the supplied EAs were N_2O, or a combination of NO_3^- and N_2O, the Shannon indices decreased to ranges of 3.2–3.4 and 3.3–3.7, respectively. The PCoA plot indicates that the influent composition changed the microbial communities in the three reactors rather than the SRT (Fig. 6A). The presence of NO_3^- separates the overlapping communities of R1 and R3 from those in R2. In the denitrification process, NO_3^- acts as the initial EA, stimulating a wide range of microbial metabolic pathways, thereby promoting the development of diverse microbial communities. In contrast, N_2O, as an intermediate product of denitrification, is also consumed by specialized microbes and may be selected for specific microbial communities [40].

Within the microbial community at the phylum level, five principal phyla were identified, including *Proteobacteria*, Firmicutes, Bacteroidota, *norank-d-Bacteria*, and *Spirochartota* (Fig. 6B). Among them, *Proteobacteria* is the predominant phylum in many heterotrophic denitrifying communities [41], with a relative abundance in R1, R2, and R3 of 70.7 %-71.9 %, 34.3 %-43.0 %, and 83.4 %-85.5 %, respectively. *Firmicutes* is also a significantly abundant phylum, 3.9 %-6.4 %, 28.5 %–32.9 %, and 2.9 %-4.4 %. Other dominant phyla, including *Bacteroidota* (1.6 %-21.6 %), *norank-d-Bacteria* (1.5 %-10.7 %), and *Spirochartota* (0.8 %-9.5 %), are closely associated with carbon/nitrogen-related metabolism and are frequently detected in various denitrification systems [42]. At the more specific order level, 14 potential denitrifying bacteria, namely *Burkholderiales*, *Pseudomonadales*, *Clostridiales*, *Vibrionales*, *Xanthomonadales*, *Caldilineales*, *Chitinophagales*, *Rhizobiales*, *Lactobacillales*, *Sphingomonadales*, *Flavobacteriales*, *Rhodobacterales*, *Rhodospirillales*, and *Pedosphaerales*, were detected (Fig. 6C, S5, S6).

Enrichment with N_2O as the sole EA increased the relative abundance of *Vibrionales*, *Clostridiales*, *Sphingomonadales*, and *Pedosphaerales* by orders of magnitude (510 % – 5304 %) compared to enrichments using NO_3^- and NO_3^- + N_2O as EAs (Fig. S6). *Vibrionales*, known as typical clade II N_2O reducers [21,43], showed an increased relative abundance, likely contributing to the elevated proportion of the *nosZ* II gene within the total bacterial community in R2. Given the widespread presence of the *nosZ* I gene in *Clostridiales* [44], the 139.5 % decrease in relative abundance in the chemostat compared to the infinite SRT period suggests that members of this order may not be well-adapted to shorter SRTs.

In addition, compared to enrichments supplied with NO_3^- and N_2O

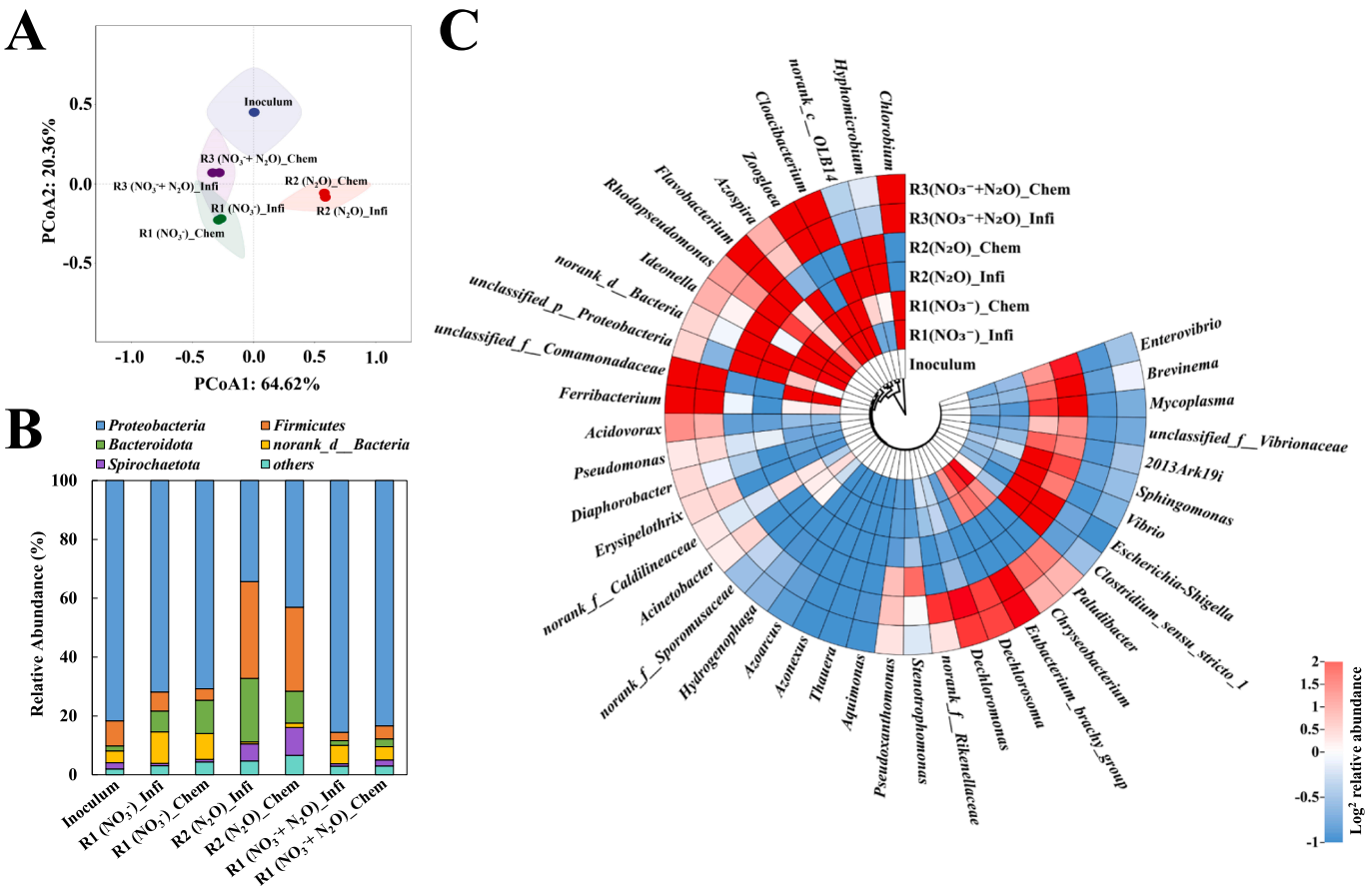

Fig. 6. PCoA of the Bray-Curtis distance (A), relative abundance of key phyla (B), and the variation in relative abundance of genera (C) in denitrifying sludge.

independently, the relative abundance of the order *Flavobacteriales* in enrichments on NO_3^- + N_2O under the two SRT modes increased by over two orders of magnitude (168 % − 479 %) (Fig. S6). Concurrently, the relative abundance of its main genus, *Flavobacterium*, also increased in R3 from 0.1 % to 4.0–4.3 %, compared to 0.1–0.2 % in R1 and 0.1–0.5 % in R2 (Fig. 6C). The genus *Flavobacterium* possesses a complete denitrification gene cluster and serves as a key microorganism responsible for N_2O reduction, capable of reducing NO_3^- to N_2 [45]. In both soil and wastewater treatment technologies this genus was enriched or correlated negatively with N_2O emissions [46–48]. The inoculation of the genus *Flavobacterium* also reduced N_2O produced by the genus *Variovorax* (which is capable of reducing NO_2^- to N_2O only) during incomplete denitrification processes [49]. Increased N_2O emissions induced by low abundance of the genus *Flavobacterium* have been observed in biological denitrification systems exposed to nano-CeO_2 and nano-TiO_2 [50,51]. Therefore, an increasing trend in the relative abundance of the genus *Flavobacterium* may predict decreasing trends in N_2O emissions. To further substantiate these observations, future studies should consider employing both metagenomics to link functional genes to assembled genomes and transcriptomic analysis to demonstrate the role of active microbes in N_2O reduction.

4. Conclusions

In this study we enriched communities using NO_3^- (R1), N_2O (R2), and NO_3^- + N_2O (R3) as sole EAs and tested their capabilities of N_2O reduction in absence or presence of other NO_x under conditions of electron competition via batch tests. The main conclusions of this study are as follows:

- Electron competition suppressed N_2O reduction rates regardless of the EA feed and SRT mode.
- The NOS enzyme is less affected under conditions of electron competition when NO_3^- + N_2O are fed simultaneously.
- *NosZ* II type N_2O-reducers enrich when N_2O serves as the sole EA, whereas *nosZ* I type N_2O-reducers are more prone to enrichment when using NO_3^- or NO_3^- + N_2O as EAs.
- The genus *Flavobacterium* plays a significant role in reducing the effect of electron competition on the N_2O consumption rate.

The competition for electrons in the N_2O consumption rate under conditions relevant for wastewater treatment would be more alleviated by bioaugmenting microbial communities fed with NO_3^- + N_2O as compared to only N_2O. Future research should explore this selective enrichment strategy to assess its effectiveness in reducing N_2O emissions in engineered systems.

CRediT authorship contribution statement

Jinyu Ye: Writing – original draft, Visualization, Methodology, Investigation. **Marlene Mark Jensen:** Writing – review & editing, Methodology. **Estelle M. Goonesekera:** Methodology. **Ran Yu:** Writing – review & editing, Supervision, Funding acquisition. **Barth F. Smets:** Writing – review & editing, Supervision, Funding acquisition, Conceptualization. **Borja Valverde-Pérez:** Writing – review & editing, Supervision, Project administration, Funding acquisition. **Carlos Domingo-Félez:** Writing – review & editing, Data curation, Conceptualization.

Declaration of competing interest

The authors declare that they have no known competing financial interests or personal relationships that could have appeared to influence the work reported in this paper.

Data availability

Data will be made available on request.

Acknowledgement

This study was funded by National Natural Science Foundation of China (42307479) and Fundamental Research Funds of Zhejian University of Science and Technology (2023QN017). From the Danish EPA – MUDP Estelle M. Goonesekera and Borja Valverde-Pérez acknowledge the support received (Project 'Det non-biologiske minirenseanlæg' Nr. 2020 – 15527), and Carlos Domingo-Félez and Barth F. Smets acknowledge the support received (Project 'Higher Environmental Performance in WastewATer systems').

Appendix A. Supplementary data

Supplementary data to this article can be found online at https://doi.org/10.1016/j.cej.2024.155292.

References

[1] D. Richardson, H. Felgate, N. Watmough, A. Thomson, E. Baggs, Mitigating release of the potent greenhouse gas N2O from the nitrogen cycle–could enzymic regulation hold the key? Trends Biotechnol. 27 (7) (2009) 388–397.
[2] IPCC, 2019 Refinement to the 2006 IPCC Guidelines for National Greenhouse Gas Inventories, (2019).
[3] X. Chen, A.T. Mielczarek, K. Habicht, M.H. Andersen, D. Thornberg, G. Sin, Assessment of full-scale N2O emission characteristics and testing of control concepts in an activated sludge wastewater treatment plant with alternating aerobic and anoxic phases, Environ. Sci. Tech. 53 (21) (2019) 12485–12494.
[4] W.G. Zumft, P.M. Kroneck, Respiratory transformation of nitrous oxide (N2O) to dinitrogen by Bacteria and Archaea, Adv. Microb. Physiol. 52 (2006) 107–227.
[5] Q. Su, C. Domingo-Félez, M.M. Jensen, B.F. Smets, Abiotic nitrous oxide (N2O) production is strongly pH dependent, but contributes little to overall N2O emissions in biological nitrogen removal systems, Environ. Sci. Tech. 53 (7) (2019) 3508–3516, https://doi.org/10.1021/acs.est.8b06193.
[6] K. Oba, T. Suenaga, M. Kuroiwa, S. Riya, A. Terada, Exploring the Functions of Efficient Canonical Denitrifying Bacteria as N2O Sinks: Implications from 15N Tracer and Transcriptome Analyses, Environ. Sci. Tech. 56 (16) (2022) 11694–11706.
[7] C. Domingo-Felez, A.G. Mutlu, M.M. Jensen, B.F. Smets, Aeration strategies to mitigate nitrous oxide emissions from single-stage nitritation/anammox reactors, Environ Sci Technol 48 (15) (2014) 8679–8687, https://doi.org/10.1021/es501819n.
[8] Y. Zhao, H. Duan, D. Erler, Z. Yuan, L. Ye, Decoupling the simultaneous effects of NO2−, pH and free nitrous acid on N2O and NO production from enriched nitrifying activated sludge, Water Res. 245 (2023) 120609.
[9] Y. Ma, A. Piscedda, A.D.L.C. Veras, C. Domingo-Félez, B.F. Smets, Intermittent aeration to regulate microbial activities in membrane-aerated biofilm reactors: Energy-efficient nitrogen removal and low nitrous oxide emission, Chem. Eng. J. 433 (2022) 133630.
[10] M. Conthe, P. Lycus, M.O. Arntzen, A.R. da Silva, A. Frostegard, L.R. Bakken, R. Kleerebezem, M.C.M. van Loosdrecht, Denitrification as an N2O sink, Water Res. 151 (2019) 381–387, https://doi.org/10.1016/j.watres.2018.11.087.
[11] Y. Liu, Y. He, F. Chen, S. Ren, T. Zhao, T. Zhu, Y. Liu, Flocs enhance nitrous oxide reduction capacity in a denitrifying biofilm-based system: Mechanism of electron competition, Chem. Eng. J. 455 (2023) 140599.
[12] Y. Pan, B.-J. Ni, Z. Yuan, Modeling electron competition among nitrogen oxides reduction and N2O accumulation in denitrification, Environ. Sci. Tech. 47 (19) (2013) 11083–11091.
[13] C. Domingo Felez, B.F. Smets, Modelling denitrification as an electric circuit accurately captures electron competition between individual reductive steps: the ASM-Electron Competition model, Environ. Sci. Tech. (2020), https://doi.org/10.1021/acs.est.0c01095.
[14] A. Ribera-Guardia, E. Kassotaki, O. Gutierrez, M. Pijuan, Effect of carbon source and competition for electrons on nitrous oxide reduction in a mixed denitrifying microbial community, Process Biochem. 49 (12) (2014) 2228–2234.
[15] Y. Liu, Y. He, S. Ren, T. Zhu, Y. Liu, Selective organic carbon enrichment influences nitrous oxide reduction by denitrifiers: electron competition insights, ACS ES&T Water 2 (7) (2022) 1265–1275.
[16] J. Chen, M. Strous, Denitrification and aerobic respiration, hybrid electron transport chains and co-evolution, Biochimica et Biophysica Acta (BBA)-Bioenergetics 1827 (2) (2013) 136–144.
[17] A. Ribera-Guardia, R. Marques, C. Arangio, M. Carvalheira, A. Oehmen, M. Pijuan, Distinctive denitrifying capabilities lead to differences in N2O production by denitrifying polyphosphate accumulating organisms and denitrifying glycogen accumulating organisms, Bioresource Technol 219 (2016) 106–113.

[18] C. Müller, L. Zhang, S. Zipfel, A. Topitsch, M. Lutz, J. Eckert, B. Prasser, M. Chami, W. Lü, J. Du, Molecular interplay of an assembly machinery for nitrous oxide reductase, Nature 608 (7923) (2022) 626–631.
[19] C. Qi, Y. Zhou, T. Suenaga, K. Oba, J. Lu, G. Wang, L. Zhang, S. Yoon, A. Terada, Organic carbon determines nitrous oxide consumption activity of clade I and II nosZ bacteria: Genomic and biokinetic insights, Water Res. 209 (2022) 117910.
[20] M. Conthe, L. Wittorf, J.G. Kuenen, R. Kleerebezem, M.C. van Loosdrecht, S. Hallin, Life on N2O: deciphering the ecophysiology of N2O respiring bacterial communities in a continuous culture, ISME J. 12 (4) (2018) 1142.
[21] M. Conthe, L. Wittorf, J.G. Kuenen, R. Kleerebezem, S. Hallin, M.C. van Loosdrecht, Growth yield and selection of nosZ clade II types in a continuous enrichment culture of N2O respiring bacteria, Environ. Microbiol. Rep. 10 (3) (2018) 239–244.
[22] S. Yoon, S. Nissen, D. Park, R.A. Sanford, F.E. Löffler, Nitrous oxide reduction kinetics distinguish bacteria harboring clade I NosZ from those harboring clade II NosZ, Appl Environ Microb 82 (13) (2016) 3793–3800.
[23] J. Juhanson, S. Hallin, M. Söderström, M. Stenberg, C.M. Jones, Spatial and phyloecological analyses of nosZ genes underscore niche differentiation amongst terrestrial N2O reducing communities, Soil Biol. Biochem. 115 (2017) 82–91.
[24] E.M. Goonesekera, P. Tsapekos, I. Angelidaki, B. Valverde-Pérez, Impact of recovered phosphorus supply on methanotrophic cultivation and microbial protein production, J. Environ. Manage. 322 (2022) 115820.
[25] S. Xu, D. Wu, Z. Hu, Impact of hydraulic retention time on organic and nutrient removal in a membrane coupled sequencing batch reactor, Water Res. 55 (2014) 12–20.
[26] J. Tang, W.J. Riley, G.L. Marschmann, E.L. Brodie, Conceptualizing biogeochemical reactions with an Ohm's law analogy, J. Adv. Model. Earth Syst. 13 (10) (2021).
[27] Z. Xia, Z. Jiang, T. Zhang, B. Liu, M. Jia, G.-H. Liu, L. Qi, H. Wang, Effects of sludge retention time (SRT) on nitrogen and phosphorus removal and the microbial community in an ultrashort-SRT activated sludge system, Environ Res 240 (2024) 117510.
[28] H. Hauduc, A. Al-Omari, B. Wett, J. Jimenez, H. De Clippeleir, A. Rahman, T. Wadhawan, I. Takacs, Colloids, flocculation and carbon capture–a comprehensive plant-wide model, Water Sci. Technol. 79 (1) (2019) 15–25.
[29] J. Jimenez, M. Miller, C. Bott, S. Murthy, H. De Clippeleir, B. Wett, High-rate activated sludge system for carbon management–Evaluation of crucial process mechanisms and design parameters, Water Res. 87 (2015) 476–482.
[30] V. Tirkey, E.M. Goonesekera, A. Kovalovszki, B.F. Smets, A. Dechesne, B. Valverde-Pérez, Short sludge age denitrification as alternative process for energy and nutrient recovery, Bioresource Technol 366 (2022) 128184.
[31] G. Liu, J. Wang, Modeling Effects of DO and SRT on Activated Sludge Decay and Production, Water Research 80 (2015) 169–178.
[32] M. Conthe, C. Parchen, G. Stouten, R. Kleerebezem, M.C. van Loosdrecht, O2 versus N2O respiration in a continuous microbial enrichment, Appl Microbiol Biot 102 (20) (2018) 8943–8950.
[33] P. Lycus, M.J. Soriano-Laguna, M. Kjos, D.J. Richardson, A.J. Gates, D.A. Milligan, Å. Frostegård, L. Bergaust, L.R. Bakken, A bet-hedging strategy for denitrifying bacteria curtails their release of N2O, Proceedings of the National Academy of Sciences 115(46) (2018) 11820-11825.
[34] Y. Pan, B.-J. Ni, P.L. Bond, L. Ye, Z. Yuan, Electron competition among nitrogen oxides reduction during methanol-utilizing denitrification in wastewater treatment, Water Res. 47 (10) (2013) 3273–3281.
[35] J.-J. Wang, B.-C. Huang, J. Li, R.-C. Jin, Multiple electron acceptor-mediated sulfur autotrophic denitrification: Nitrogen source competition, long-term performance and microbial community evolution, Bioresource Technol 329 (2021) 124918.
[36] R. Shukla, S.Z. Ahammad, Performance evaluation and microbial community structure of a modified trickling filter and conventional activated sludge process in treating urban sewage, Sci. Total Environ. 853 (2022) 158331.
[37] D.R. Graf, C.M. Jones, S. Hallin, Intergenomic comparisons highlight modularity of the denitrification pathway and underpin the importance of community structure for N2O emissions, PLoS One 9 (12) (2014) e114118.
[38] X. Li, R. Zhao, D. Li, G. Wang, S. Bei, X. Ju, R. An, L. Li, T.W. Kuyper, P. Christie, Mycorrhiza-mediated recruitment of complete denitrifying Pseudomonas reduces N2O emissions from soil, Microbiome 11 (1) (2023) 1–18.
[39] S. Hallin, L. Philippot, F.E. Löffler, R.A. Sanford, C.M. Jones, Genomics and ecology of novel N2O-reducing microorganisms, Trends Microbiol 26 (1) (2018) 43–55.
[40] M.M.M. Kuypers, H.K. Marchant, B. Kartal, The microbial nitrogen-cycling network, Nat. Rev. Microbiol. 16 (5) (2018) 263–276, https://doi.org/10.1038/nrmicro.2018.9.
[41] Y. Zhou, C. Wang, X. Xu, W. Jin, L. Liu, F. Meng, F. Yang, Deciphering the partial denitrification function of companion bacteria in mixotrophic anammox systems under different carbon/nitrogen ratios, J. Environ. Chem. Eng. 11 (6) (2023) 111232.
[42] X. Wu, Z. Yu, S. Yuan, A. Tawfik, F. Meng, An ecological explanation for carbon source-associated denitrification performance in wastewater treatment plants, Water Res. 247 (2023) 120762.
[43] M. Bandekar, N. Ramaiah, S.C. Seleyi, D.R. Nazareth, J. Kekäläinen, Diversity and Quantitative Detection of Clade I Type nosZ Denitrifiers in the Arabian Sea Oxygen Minimum Zone, Microbes Environ. 38 (1) (2023) ME22056.
[44] P.A. Calderoli, F.J. Espinola, H.M. Dionisi, M.N. Gil, J.K. Jansson, M. Lozada, Predominance and high diversity of genes associated to denitrification in metagenomes of subantarctic coastal sediments exposed to urban pollution, PLoS One 13 (11) (2018) e0207606.
[45] M. Conthe, J.G. Kuenen, R. Kleerebezem, M.C. van Loosdrecht, Exploring microbial N2O reduction: a continuous enrichment in nitrogen free medium, Environ. Microbiol. Rep. 10 (1) (2018) 102–107.
[46] H. Yoon, M.J. Song, D.D. Kim, F. Sabba, S. Yoon, A serial biofiltration system for effective removal of low-concentration nitrous oxide in oxic gas streams: mathematical modeling of reactor performance and experimental validation, Environ. Sci. Tech. 53 (4) (2019) 2063–2074.
[47] W. Mao, R. Yang, H. Shi, H. Feng, S. Chen, X. Wang, Identification of key water parameters and microbiological compositions triggering intensive N2O emissions during landfill leachate treatment process, Sci. Total Environ. 833 (2022) 155135.
[48] J. Harter, P. Weigold, M. El-Hadidi, D.H. Huson, A. Kappler, S. Behrens, Soil biochar amendment shapes the composition of N2O-reducing microbial communities, Sci. Total Environ. 562 (2016) 379–390.
[49] E.R. Hester, M. Sekulić, L. Bergaust, L.R. Bakken, M.S. Jetten, C. Welte, S. Lücker, Interplay of complete and partial denitrifying bacteria mitigates NO and N, Metabolic interactions in the rhizosphere: from ecology to physiology (2019) 125.
[50] J. Ye, H. Gao, C. Domingo-Félez, J. Wu, M. Zhan, R. Yu, B.F. Smets, Chronic effects of cerium dioxide nanoparticles on biological nitrogen removal and nitrous oxide emission: Insight into impact mechanism and performance recovery potential, Bioresource Technol (2022) 126966. 10.1016/j.biortech.2022.126966.
[51] J. Ye, H. Gao, J. Wu, G. Yang, L. Duan, R. Yu, Long-term exposure to nano-TiO2 interferes with microbial metabolism and electron behavior to influence wastewater nitrogen removal and associated N2O emission, Environ Pollut 311 (2022) 119930.